JJEES

JJEES (2021) 12 (2): 122-133
ISSN 1995-6681

Jordan Journal of Earth and Environmental Sciences

# Treatment of real olive mill wastewater by sole and combination of $H_2O_2$, $O_3$, and UVA: effect of doses and ratios on organic content and biodegradability

Dheaya Alrousan

*Department of Water Management and Environment, Prince EL-Hassan Bin Talal Faculty for Natural Resources and Environment, The Hashemite University, Jordan.*

*Received 8 October 2020; Accepted 25 October 2020*

**Abstract**

Given the rapidly growing olive oil agroindustry, many countries in the coming future will face the same challenge of olive mill wastewater (OMW) management as the Mediterranean countries currently do. Ozonation and ozone-based advanced oxidation processes (AOPs) could represent a promising complementary or alternative solution for OMW treatment. One critical parameter that significantly influences the efficiency and the cost of ozone processes is the chemical dosages and ratios. This research investigated OMW treatment by sole and combination of $H_2O_2$, $O_3$, and UVA irradiation, in a glass tube photoreactor and by applying a wide range of $H_2O_2$ and $O_3$ dosages and ratios. The treatment efficiency was evaluated based on the reduction of dissolved organic carbon (DOC) and the change in biodegradable organic content expressed by $BOD_5$ and biodegradability. The highest DOC reduction in this study was ≈ 40% by UVA/ peroxonation, while the highest enhancement in $BOD_5$ (209%) and biodegradability (254%) was achieved by dark peroxonation. However, a wide range of doses combination can result in the same degree of change in DOC reduction or $BOD_5$ and biodegradability enhancement. This lab-based study demonstrates the potential of the studied systems to significantly reduce the organic fraction of real OMW and increase the biodegradability, which offering a new spectrum to optimize the chemical dosages based on the purpose of the treatment.



**Keywords:** Olive mill wastewater, ozonation, peroxonation, biodegradability, AOPs

## 1. Introduction

The countries around the Mediterranean basin hold 97% of global olive oil production (Saez et al., 2020). Unfortunately, high production is always combined with large quantities of wastewater as a byproduct, where around 30 million $m^3$ of olive mill wastewater (OMW) is generated annually in the Mediterranean region alone (Pedrero et al., 2020). Even though the OMW amount is not relatively high, most countries' legislations prohibits OMW's direct discharge in water bodies (Al-Bsoul et al., 2020). Still, whenever that happened, it has caused catastrophic environmental consequences due to the high OMW pollution impact, which is assumed to be 100 – 200 times to that of the domestic wastewater (El-Abbassi et al., 2013). Moreover, the amount of OMW generated worldwide is expected to increase in the coming future because of the rapidly growing agroindustry of olive oil production in countries outside the Mediterranean, such as Argentina, Australia, and Chile (Pedrero et al., 2020).

The OMW characteristics are affected by several factors, such as olive type, degree of fruit maturity, and the oil extraction method (Erses Yay et al., 2012). However, it is generally characterized by a dark brown color, unpleasant odor, low pH, high organic and suspended solids content, and similarly high levels of phenolic compounds (Ioannou-Ttofa et al., 2017; Ahmed et al., 2019). The simplest and most common practices followed for OMW treatment at low cost, and unskilled labor are evaporation ponds. Despite the suitability of evaporation ponds in the Mediterranean countries where the evaporation rates are high during the summer period, the leakages and infiltration into groundwater, in addition to odor and breading of insects, are some of evaporation ponds disadvantages (Saez et al., 2020; Erses Yay et al., 2012; Khoufi et al., 2009). In the context of; i) the high organic and phenolic content of OMW, ii) the seasonal OMW generation during a few months of the year, iii) and the geographically scattering of the olive mills (Ioannou-Ttofa et al., 2017; Ahmed et al., 2019), different treatment methods have been considered to overcome those limitations, which includes, but not limited to, electrocoagulation (Niazmand et al., 2020), membrane processes (Akdemir and Ozer, 2009), adsorption (Azzam et al., 2013), electrocatalysis (UĞUrlu et al., 2019), and biological treatment (Bertin et al., 2004). Unfortunately, most of the proposed OMW treatment processes are either inefficient or cost-ineffective (Ochando-Pulido et al., 2017).

In the last two decades, several remarkable studies have addressed the application of advanced oxidation processes (AOPs) for OMW treatment in particular (Al-Bsoul et al., 2020; Iboukhoulef et al., 2019; Hodaifa et al., 2019; García and Hodaifa, 2017). The key advantage of AOPs over other treatment options is their ability to non-selectively degrade various types of organic and inorganic compounds rather

* Corresponding author e-mail: dheaya@hu.edu.jo

than transform them into another phase by relying on hydroxyl radicals ($OH^{\bullet}$) formation (Ioannou-Ttofa et al., 2017; Pérez-Lucas et al., 2020). Despite the widespread use of ozone for water and wastewater treatment, a limited number of studies considered the use of ozone and ozone-based AOPs for OMW treatment (Iboukhoulef et al., 2019; Bar Oz et al., 2018) (Miranda et al., 2001; Al-Bsoul et al., 2020; Lafi et al., 2009). Nevertheless, considering the in situ costs of ozone generation, ozonation is not generally advised as a standalone solution for reducing organic content (Daghrir et al., 2016). However, combining ozone with irradiation or hydrogen peroxide ($H_2O_2$) is well reported to enhance treatment efficiency (Oturan and Aaron, 2014; Bethi et al., 2016; Li et al., 2015). The critical parameters to be optimized that are significantly influencing the efficiency and cost are the chemical dosages and the OMW organic content. The optimization depends on the treatment's purpose, which could be; 1) reducing the organic content if high purity effluent water is needed or there are restrictions on the effluent dissolved organic load, 2) or increasing the biodegradability and the biodegradable fraction for biogas production, or as a complementary step for biological treatment.

This study aims to examine the efficiency of ozone-based AOPs to treat real OMW and experimentally determine the optimum oxidants dosages and initial dissolved organic carbon concentration in the light of organic content reduction and biodegradability enhancement. The AOPs that are particularly examined in this study are $O_3$/dark, $O_3$/UVA, $H_2O_2$/dark, $H_2O_2$/UVA, $O_3/H_2O_2$, and $O_3/H_2O_2$/UVA.

## 2. Theory

Ozone has a high oxidation potential (Barzegar et al., 2019) and can attack organic compounds either directly (ozonolysis) by oxidizing particular organic compounds or indirectly by generating $OH^{\bullet}$ (Pérez-Lucas et al., 2020). The $O_3$ attack mode depends on the treatment conditions such as the pH and the organic and inorganic constituents. In ozonolysis, $O_3$ selectively attack organic compounds that have high electron density sites (Pérez-Lucas et al., 2020), such as the carbon-carbon double bond, aromatic rings, and the functional groups containing nitrogen (N), oxygen (O), sulfur (S), and phosphorus (P) (Michael-Kordatou et al., 2018). The ozonolysis reactions include the oxidation-reduction, dipolar cycloaddition, electrophilic substitution, and nucleophilic addition (Dai et al., 2015). Those reactions transform organic compounds into smaller molecular weight saturated intermediates rather than leading to full mineralization (Iboukhoulef et al., 2019). Regardless of numerous suggested reaction pathways for the indirect ozone mode of action to generate $OH^{\bullet}$, there is a general agreement that the hydroxide ions ($OH^-$) initiate the $O_3$ decomposition chain (natural decomposition) (Equation 1) (Oturan and Aaron, 2014). However, this is only true in pure water as other various compounds or actions can act as initiators of $O_3$ decomposition, which can be generalized in the form of Equation 2 (chemically assisted decomposition). The decomposition initiators include but not limited to, humic substances, formate (Gardoni et al., 2012), transition metal ions (Kasprzyk-Hordern et al., 2003), activated carbon (Farzadkia et al., 2014), phenols and amines (Wert et al., 2009), and UV irradiation (UV photo-ozonation) in the range of 200 – 360 nm (Equation 3) (Oturan and Aaron, 2014; Bustos-Terrones et al., 2016).

$$3O_3 + OH^- + H^+ \rightarrow 2OH^{\bullet} + O_3^{\bullet -} + 4O_2 \quad \text{Eq. 1}$$

$$O_3 + H_2O + \text{decomposition initiator} \rightarrow \text{series of reactions} \rightarrow OH^{\bullet} \quad \text{Eq. 2}$$

$$O_3 + H_2O + h\nu \rightarrow 2\,OH^{\bullet} + O_2 \quad \text{Eq. 3}$$

Hydrogen peroxide, in particular, gained huge interest as $O_3$ decomposer (Equation 4) (researchers often name this process by peroxonation, wet peroxide ozonation, and perozonation) (Miklos et al., 2018; Oturan and Aaron, 2014; Li et al., 2015; Englehardt et al., 2013). The peroxonation process utilizes the direct ozone and hydrogen peroxide oxidation power and the generated hydroxyl radicals' mineralization capability.

$$2O_3 + H_2O_2 \rightarrow 2OH^{\bullet} + 3O_2 \quad \text{Eq. 4}$$

Even though $H_2O_2$ is considered as relatively inexpensive and environmentally friendly oxidant, it has limited application as sole organic content reduction because of its weak oxidation potential (Oturan and Aaron, 2014). However, similar to ozone, $H_2O_2$ can be decomposed to generate hydroxyl radicals where this decomposition can be initiated and promoted by; transitional metals (Fe, Cu, Co, etc.) (Yazdanbakhsh et al., 2015), activated carbon (Kurniawan and Lo, 2009), $TiO_2$ (Moreira et al., 2018), zero-valent iron (ZVI) (Yazdanbakhsh et al., 2015) and UV irradiation in the range of 200 to 300 nm (Equation 5) (Oturan and Aaron, 2014).

$$H_2O_2 + h\nu \rightarrow 2\,OH^{\bullet} \quad \text{Eq. 5}$$

The peroxonation process efficiency can be further improved by combining it with UV irradiation (UV peroxonation), which boosts the $OH^{\bullet}$ generation (Hassanshahi and Karimi-Jashni, 2018; Bethi et al., 2016; Wang and Xu, 2012). In most of the studies, the employed UV is high energy and short wavelength source such as; UVC (Guo et al., 2018), UV-ABC (Antonio da Silva et al., 2018), VUV (Yuval et al., 2017), UVAB (Huang et al., 2018), and gamma irradiation (Ebrahimi et al., 2018) with limited interest in using the near-ultraviolet irradiation (Nie et al., 2010; Dong et al., 2019; Celeiro et al., 2018).

One critical parameter in ozone-based AOPs are the oxidants dosages, as using inappropriate doses of $H_2O_2$ or $O_3$ may act as hydroxyl radicals scavenger (Equation 6 (Elmolla and Chaudhuri, 2010) and Equation 7 (Barzegar et al., 2019)) by reacting with the very reactive hydroxyl radicals ($OH^{\bullet}$) ($E^0$ = 2.8 V) (Yazdanbakhsh et al., 2015) and producing the less reactive hydroperoxyl radicals () ($E^0$ = 1.7 V ) (Kurniawan and Lo, 2009). The hydroperoxyl radicals have even lower oxidation power than ozone ($E^0$ = 2.07 V) (Barzegar et al., 2019) or hydrogen peroxide ($E^0$ = 1.78 V) (Oturan and Aaron, 2014).

$$H_2O_2 + OH^{\bullet} \rightarrow HO_2^{\bullet} + H_2O \quad \text{Eq. 6}$$

$$O_3 + OH^{\bullet} \rightarrow HO_2^{\bullet} + O_2 \quad \text{Eq. 7}$$

## 3. Material and methods

### 3.1. Olive mill wastewater

OMW in this study was obtained during the milling campaign of 2017/2018 from Al Zyoud Olive Oil Mill, located in Alzarqa (middle – north of Jordan) that uses a three-phase continuous olive oil extraction (Rapanelli International, Italy). Fresh samples of OMW were collected from the decenter outlet in 20 L polyethylene containers, transferred to the laboratory within 20 min, filtered through a 0.45 µm membrane, and stored at 3-5 ℃. The main physicochemical characteristics of the filtered OMW are summarized in Table 1.

**Table 1.** Olive mill wastewater characteristics

| parameter | unit | Value ± Standard deviation |
|---|---|---|
| Chemical oxygen demand (COD) | mg/L | 38750 ± 320 |
| Biochemical oxygen demand ($BOD_5$) | mg/L | 2221 ± 160 |
| Dissolved organic carbon (DOC) | mg/L | 11413.4 ± 373.8 |
| Total solids (TS) | mg/L | 41870 ± 770 |
| Total suspended solids (TSS) | mg/L | 28350 ± 460 |
| pH | - | 4.52 ± 0.38 |
| Conductivity | mS/cm | 10.4 ± 0.25 |
| Turbidity | NTU | 57.8 ± 3.52 (NTU) |

### 3.2. Materials

All chemicals used were of high purity grade and sourced from Sigma Aldrich and BDH. For TOC standards preparation, potassium hydrogen phthalate was supplied by Nacalai Tesque Inc. Hydrogen peroxide 35% strength was supplied by BDH, AnalaR. Ozone was produced in situ using OZ-3G ozone generator (Ozonefac Ltd., China) with a variable ozone outlet concentration and a constant air flow rate of 5 L/min.

### 3.3. Analytical methods

The treatment efficiency was evaluated by measuring the dissolved organic carbon (DOC) and the biochemical oxygen demand ($BOD_5$). DOC was used rather than the chemical oxygen demand (COD) to minimize hydrogen peroxide interference with COD measurements (Elmolla and Chaudhuri, 2010), and was evaluated using Shimadzu 5000 TOC/V with auto-sampler. The injected sample volume was 50 µL, and the catalyst used was the regular sensitivity Pt catalyst. The samples' biodegradable organic content was determined by measuring the $BOD_5$ using $BOD_5$ EVO System 6 (VELP Scientifica, Inc). The $BOD_5$ samples have all been subjected to extended aeration in the dark for 15 min before being tested to avoid any measurements interfering caused by ozone residue. All samples in this study were analyzed in triplicate unless otherwise stated.

### 3.4. Experimental setup

The experiments were carried out in a custom-built borosilicate glass tube photoreactor with concentrated parabolic collectors (Figure 1). Full details of the photoreactor modules are described in our previous publication (Alrousan and Dunlop, 2020). Even the reactor was initially designed for experiments under solar irradiation; it was used with artificial UVA lamps in this study for future research comparison purposes.

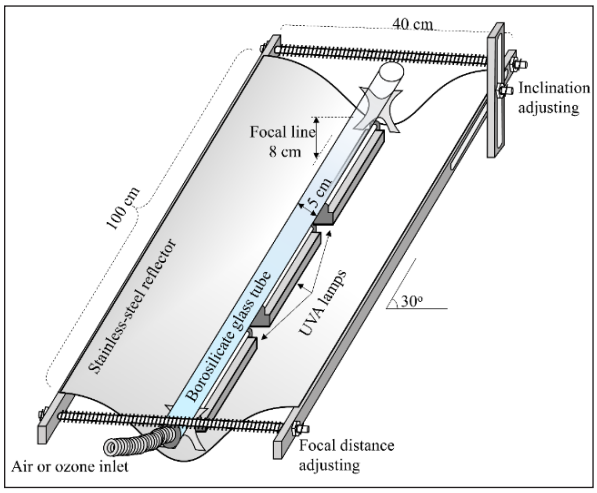


**Figure 1.** Glass tubes photoreactor with concentrated parabolic collectors

The photoreactor was illuminated from below using three 11W UVA lamps (TL11W/05 Philips lamp, Holland). The lamps emitted radiation between 300 – 460 nm with maximum emission at 365 nm and average incident UVA intensity of 55.4 ± 6.3 W/m$^2$. The glass tube total capacity is 1.96 L; however, due to the inclination angle and to ensure room for gas bubbling, the volume of OMW treated in each experimental batch was 1.5 L. The glass tube was wrapped in aluminum foil for studies without irradiation. Depending on the experiments' purpose, air or air with ozone was continuously fed to the tube reactor. For experiments with hydrogen peroxide, hydrogen peroxide was added as a single dosage to the OMW at the beginning of each experiment with different concentrations. OMW was diluted with distilled water to give initial DOC concentration from 1000 - 4000 mg/L (corresponds to $DOC_0$ of 83.3 – 333.3 mM). All experiments were carried out for three hours, and 500 ml samples were withdrawn before and after the treatment for physiochemical analysis. Table 2 describes the systematic approach to the experimental conditions.

**Table 2.** Matrix of experimental conditions.a

| Experiment | $O_3$ dosage (mM) | $H_2O_2$ dosage (mM) | Illumination conditions |
|---|---|---|---|
| Dark/aerated | 0.00 | 0.00 | dark |
| UVA/aerated | 0.00 | 0.00 | UVA |
| Ozonation ($O_3$/dark) | 37.5 -150 | 0.00 | dark |
| Ozone photolysis ($O_3$/UVA) | 37.5 -150 | 0.00 | UVA |
| $H_2O_2$-peroxidation ($H_2O_2$/dark) | 0.00 | 66.7 -266.7 | dark |
| ($H_2O_2$/UVA) | 0.00 | 66.7 -266.7 | UVA |
| Peroxonation ($H_2O_2$/$O_3$/dark) | 37.5 -150 | 66.7 -266.7 | dark |
| Photo-peroxonation ($H_2O_2$/$O_3$/UVA) | 37.5 -150 | 66.7 -266.7 | UVA |

[a] The nominal DOC0 for all experiments ranged from (83.3 – 333.3 mM), real values were slightly different from that

### 3.5. Calculations and data representation

The biodegradability (abbreviated as Bio) was represented by the ratio of $BOD_5$ to DOC values, as expressed in Equation 8.

$$Bio = \frac{BOD_5}{DOC}$$

The change in TOC, $BOD_5$, and biodegradability was expressed in normalized form as in the general Equation 9, where $M_0$ and $M_f$ are the measured values before and after the treatment, respectively.

$$E_M = \frac{M_f}{M_0} \quad \text{Eq. 9}$$

The independent variables; $H_2O_2$ dosage, $O_3$ dosage, and the initial dissolved organic carbon ($DOC_0$) of the tested OMW, were normalized in the form of a molar fraction (X) by dividing the value of each independent variable (measured by mM) by the summation of all independent variables (Equation 10 - Equation 12).

$$X_{H_2O_2} = \frac{H_2O_2\ dosage}{H_2O_2\ dosage + O_3\ dosage + DOC_0} \quad \text{Eq. 10}$$

$$X_{O_3} = \frac{O_3\ dosage}{H_2O_2\ dosage + O_3\ dosage + DOC_0} \quad \text{Eq. 11}$$

$$X_{DOC_0} = \frac{DOC_0}{H_2O_2\ dosage + O_3\ dosage + DOC_0} \quad \text{Eq. 12}$$

All 3D plots were created using Origin 2019b software (OriginLab Corporation, Northampton, USA) with a built-in Thin Plate Spline (TPS) algorithm.

## 4. Results and discussion

### 4.1. Control experiments

In control experiments, diluted OMW with various initial organic content was subjected for three hours to different light exposure conditions (dark and UVA irradiation) with and without aeration. No change in OMW organic content was noticed for experiments without aeration, even under UVA irradiation (data not shown). As can be observed from Figure 2a, there was a very slight reduction in DOC and $BOD_5$ (≈ 1.4% and ≈ 3.6%, respectively) under dark aeration conditions with almost no effect of the initial OMW organic content ($DOC_0$). However, there is no reason for this tiny reduction except the air stripping of the purgeable dissolved organic carbon (PDOC), such as the volatile and low boiling organic compounds, which are commonly found in OMW and cause odor problems in the vicinities of the olive mills (Azbar et al., 2004). Based on the relatively higher reduction in $BOD_5$ compared to DOC, it can be assumed that the bulk of PDOCs in the studied OMW are biodegradable compounds.

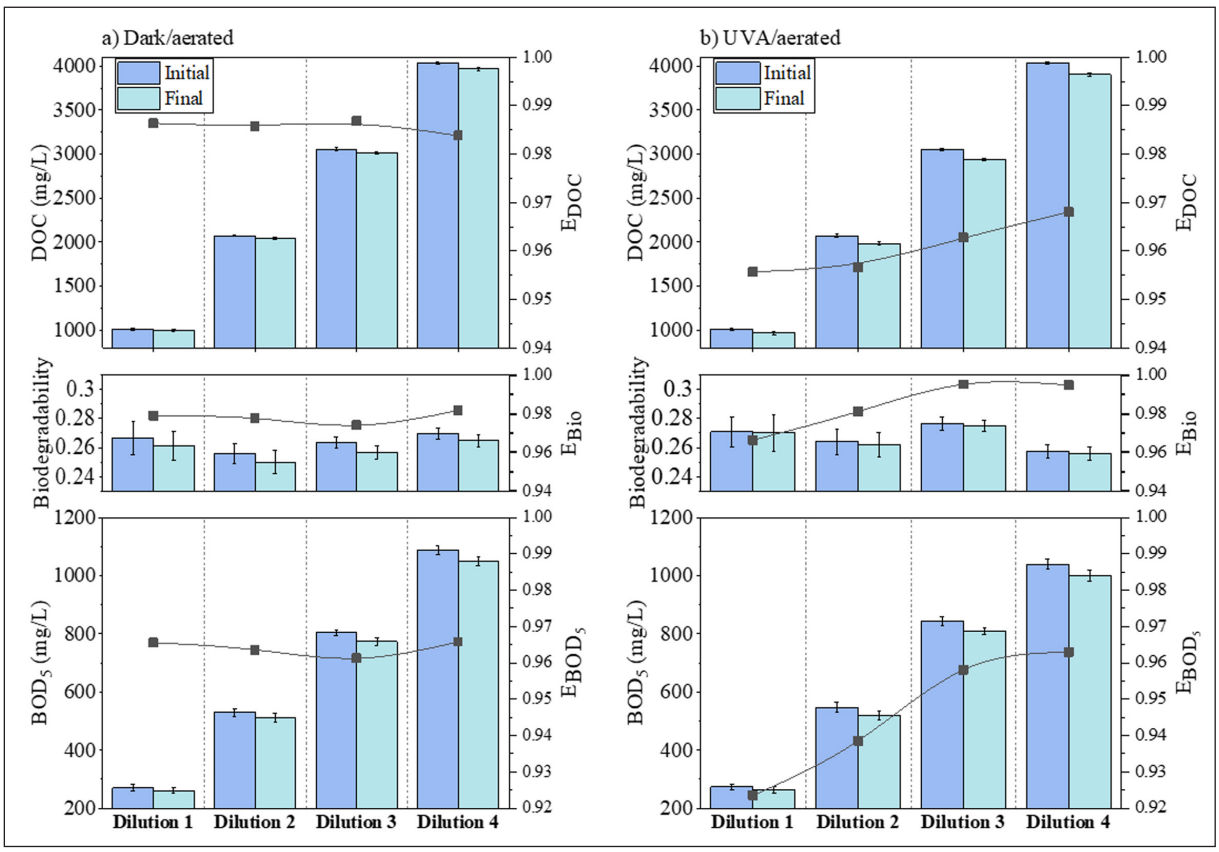


**Figure 2.** Change in DOC, biodegradability, and BOD5 using different OMW dilutions under dark and UVA aeration.

Referring to Figure 2b, the DOC and $BOD_5$ reduction (Max. ≈ 4.4% and ≈ 7.6%, respectively) became more than twice under UVA irradiation compared to those in the dark. This enhancement might be accredited to OMW organics' photolytic decomposition or the air stripping of the photolytic decomposition intermediates. It is well proven that organic compounds, most of the time, are more subjected to photolysis (Antonio da Silva et al., 2018). Furthermore, olive oil is well reported to contain natural photosensitizers (Ali et al., 2020), and so expected the wastewater generated from the extraction process. Even increasing $DOC_0$ is expected to amplify the degradation by providing more photosensitizers; it was found to slightly reduce the $E_{DOC}$ and $E_{BOD5}$, which could be linked to the light penetration reduction (Nguyen and Juang, 2015). According to García and Hodaifa (García and Hodaifa, 2017), one of the critical barriers for UV penetration in OMW is the turbidity. Regardless of the photolysis capability to affect the organic content in different wastewaters (industrial, municipal, and greywater) (Gulyas et al., 2005), the findings in this study are in agreement with the reported insufficiency of photolysis to promote the pollutants mineralization even at a higher intensity or longer irradiation time (Moreira et al., 2018; Otálvaro-Marín et al., 2019).

### *4.2. Ozonation and ozone photolysis*

ozonation and ozone photolysis have been evaluated at different $O_3$ doses (37.5-150 mM) and $DOC_0$ values (83.3 to 333.3 mM). The change in DOC, $BOD_5$, and biodegradability in this section was represented graphically by 3D surface plots as a function of $O_3$ dosage and $DOC_0$ value (shown in the graphs insets), and 2D plots as a function of ozone dosage molar fraction ($X_{O3}$). Although it is not widely common in AOPs to represent the results as a function of oxidant molar fraction, it was found to be an excellent parameter to explain the findings in this study, as will be seen. A similar, but not exact conclusion was drawn by Buffle et al. (Buffle et al., 2006), who investigated the effect of ozone dose on wastewater treatment from different sources and found the efficiency better described by the ozone molar ratio ($O_3$ dosage/$DOC_0$).

#### *4.2.1. Organic content reduction ($E_{DOC}$)*

As can be observed from Figure 3 a and b, ozonation and ozone photolysis showed a higher DOC reduction in comparison to the corresponding control experiments (dark/aerated and UVA/aerated) in the previous section, where 10% and 17% DOC reduction by ozonation and UVA ozonation, respectively, been achieved under the best conditions.

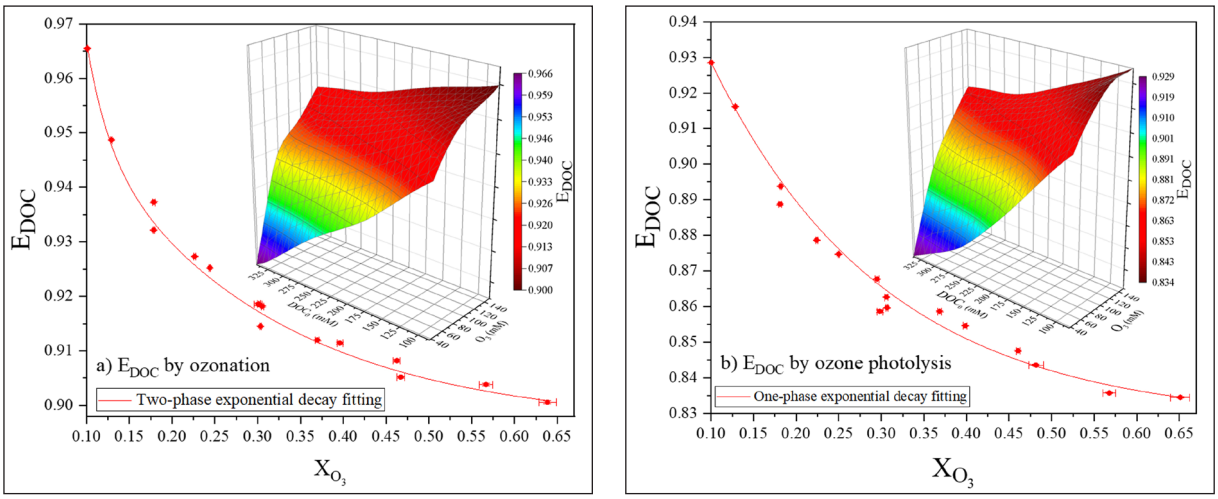


**Figure 3.** Effect of $O_3$ dosage molar ratio ($X_{O3}$) on DOC reduction ($E_{DOC}$) by; a) ozonation and b) ozone photolysis, the insets show the 3D surface plots of $E_{DOC}$ as a function of $O_3$ dosage and $DOC_0$ value.

In general, the efficiency of all AOPs that are combined with aeration is linked to at least three mechanisms: 1) complete mineralization, 2) air stripping of the purgeable intermediates, and 3) air stripping of the unoxidized starting organics (< 1.4% in this study). In ozone-based processes, in particular, the first two mechanisms are dependent on direct ozone oxidation, and $OH^{\bullet}$ generated from ozone decomposition (natural (Equation 1), chemically assisted (Equation 2), and photo-assisted (Equation 3)). Indeed natural ozone decomposition favors alkaline conditions (Oturan and Aaron, 2014), which is not the situation in this study (pH of OMW = 4.52 ± 0.38). However, various constitutes present in OMW may initiate $O_3$ decomposition, as explained before. In addition to the $OH^{\bullet}$ provided by photo-assisted ozone decomposition (Equation 3), organic photolysis should not be neglected as it showed a significant effect in UVA/aerated control experiments.

As shown in Figure 3 insets, $E_{DOC}$ is reduced by either increasing the $O_3$ dosage or reducing the $DOC_0$. According to the literature, there is a general agreement that increasing ozone dose will lead to a higher degree of degradation (Daghrir et al., 2016; Bustos-Terrones et al., 2016; Khataee et al., 2017). However, there are different opinions about the effect of the initial pollutant concentration, where some authors reported an increase in degradation with higher DOC (Bustos-Terrones et al., 2016), and some others reported the opposite (Khataee et al., 2017). Nevertheless, the effect of both parameters ($O_3$ dose and $DOC_0$) on $E_{DOC}$ can be interlinked by their ratio represented by ozone dosage molar fraction ($X_{O3}$). The appropriateness of $X_{O3}$ can be noticed by the low scattering of equal ratio points in Figure 3. As can be observed, the low range $X_{O3}$ showed a higher impact on DOC reduction than the high range. Increasing $X_{O3}$ from 0.1 to 0.3, for instance, reduced $E_{DOC}$ by 5% and

7% in ozonation and ozone photolysis, respectively. On the other hand, doubling $X_{O3}$ from 0.3 to 0.6 did not reduce $E_{DOC}$ by more than 3% in either system. The decay in $E_{DOC}$ by increasing $X_{O3}$ is attributed to $OH^{\bullet}$ scavenging induced by excessive ozone ratio (Equation 7) (Barzegar et al., 2019) or by the inorganic constitutes of OMW that are reported by authors to act as $OH^{\bullet}$ scavengers (such as , and) (Kasprzyk-Hordern et al., 2003; Al-Bsoul et al., 2020). Another hypothesis explained by Li et al. (Li et al., 2015) is related to the degradation process being controlled by the dissolved $O_3$ concentration in water rather than $O_3$ fed to the system. Still, the organic content reduction in this study was lower than that reported elsewhere regarding OMW by ozonation ((Lafi et al., 2009; Iboukhoulef et al., 2019) or UV/ozonation (Lafi et al., 2009; Miranda et al., 2001). Variation in DOC reduction effectiveness among studies is mainly associated with the water matrix components, the ozone dosage, and the UV source. Unfortunately, no studies examined OMW degradation by ozone under UVA irradiation up to our knowledge. Previous studies of the cited literature (Lafi et al., 2009; Miranda et al., 2001) have used high energy low wavelength light sources in their work.

The $E_{DOC}$ in ozonation (Figure 3a) and ozone photolysis (Figure 3b) could be modeled by a two-phase exponential decay relationship of $X_{O3}$ (Equation 13). However, the ozone photolysis can be simplified to a one-phase exponential decay with a correlation coefficient ($R^2$) higher than 0.98. The fitting parameters are shown in Table 3.

$$EDOC = \alpha + \beta_1 e^{-\left(\frac{X_{O3}}{k_1}\right)} + \beta_2 e^{-\left(\frac{X_{O3}}{k_2}\right)} \quad \text{Eq. 13}$$

Where α represents the offset, $\beta_1$ and $\beta_2$ are phase 1 and 2 amplitudes, and $k_1$ and $k_2$ are phase 1 and 2 ratio constants, respectively.

**Table 3.** Two-phase exponential decay fitting parameters for ozonation and ozone photolysis

| Parameters/system | ozonation | ozone photolysis |
|---|---|---|
| α | 0.896 | 0.828 |
| $\beta_1$ | 0.934 | 0.165 |
| $k_1$ | 0.025 | 0.204 |
| $\beta_2$ | 0.082 | - |
| $k_2$ | 0.220 | - |
| $R^2$ | 0.981 | 0.987 |

#### *4.2.2. Change in $BOD_5$ and biodegradability*

In ozonation, $E_{BOD5}$ showed low and high optimum values with respect to ozone dosage and initial organic content. Those values were corresponding to 0.15 and 0.45 $X_{O3}$ (Figure 4a). The change in BOD5 (either reduction or enhancement) describes the net difference between the biodegradable intermediates remain in the water and the biodegradable organics that escape the water, entirely (in the form of $CO_2$ and $H_2O$) or partially mineralized (purgeable and volatile intermediates). In the light of DOC reduction, it is possible to assume that the first fraction of organic components in OMW to be attacked by ozone are the easily biodegradable compounds such as amino acids, simple carbohydrates, and fats. For low $X_{O3}$ values (< 0.15), the ozone attack causes higher actual mineralization or more purgeable intermediates than causing biodegradable intermediates accumulation. By increasing $X_{O3}$ above 0.15, refractory organics break down and become more biodegradable but with very low reactivity toward ozone, leading to the accumulation of biodegradable intermediates (Antonio da Silva et al., 2018). Similar findings have been reported by Andreozzi et al. (Andreozzi et al., 2008) when they investigated OMW treatment by ozone. In that study, treating OMW for 1 hr by ozone reduced the phenolic content by 56.8% while the COD reduction did not exceed 8.1%. Despite the presence of low optimum $E_{BOD5}$, no similar optimum value was noticed for $E_{Bio}$ (Figure 4b) as the $E_{DOC}$ reduction effect dumped it in that $X_{O3}$ range. At $X_{O3}$ > 0.45, $BOD_5$ and biodegradability become inversely proportional to $X_{O3}$, but to a lesser degree than their rising rate. Several authors referred that to the formation of biorecalcitrant intermediates (Amor et al., 2019).

In UVA ozonation, $BOD_5$ and biodegradability (Figure 5 a and b) increased by increasing the $O_3$ to $DOC_0$ ratio without showing any optimum value. This phenomenon of biodegradability enhancement by ozone photolysis is widely reported in the literature (Yazdanbakhsh et al., 2015; Bar Oz et al., 2018) and attributed to the accumulation of the biodegradable intermediate as explained.

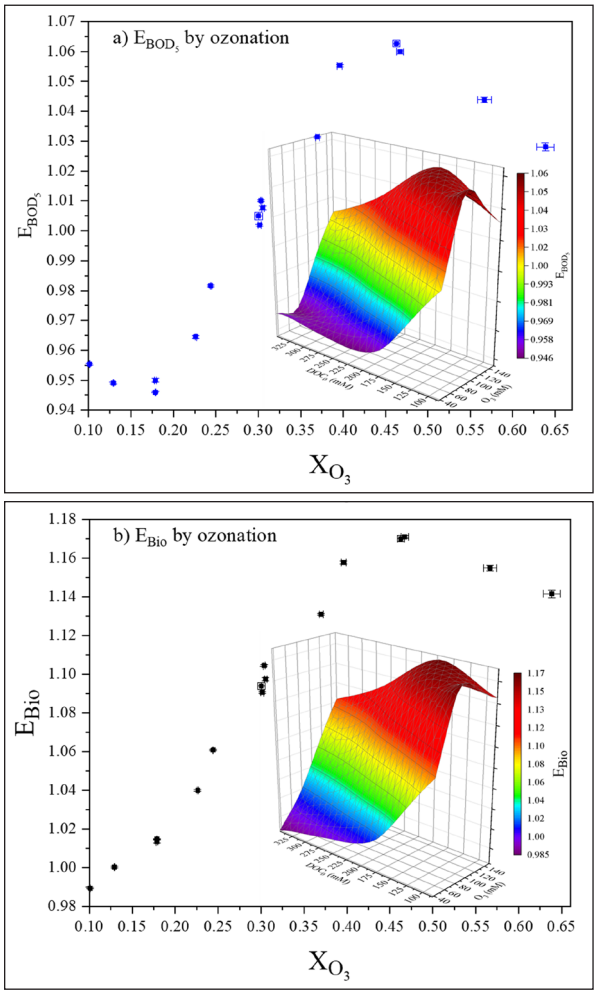


**Figure 4.** Effect of $O_3$ dosage molar ratio ($X_{O3}$) on the change of $BOD_5$ ($E_{BOD5}$) and biodegradability ($E_{bio}$) by ozonation, the insets show the 3D surface plots of $E_{BOD5}$ and $E_{bio}$ as a function of $O_3$ dosage and $DOC_0$ value.

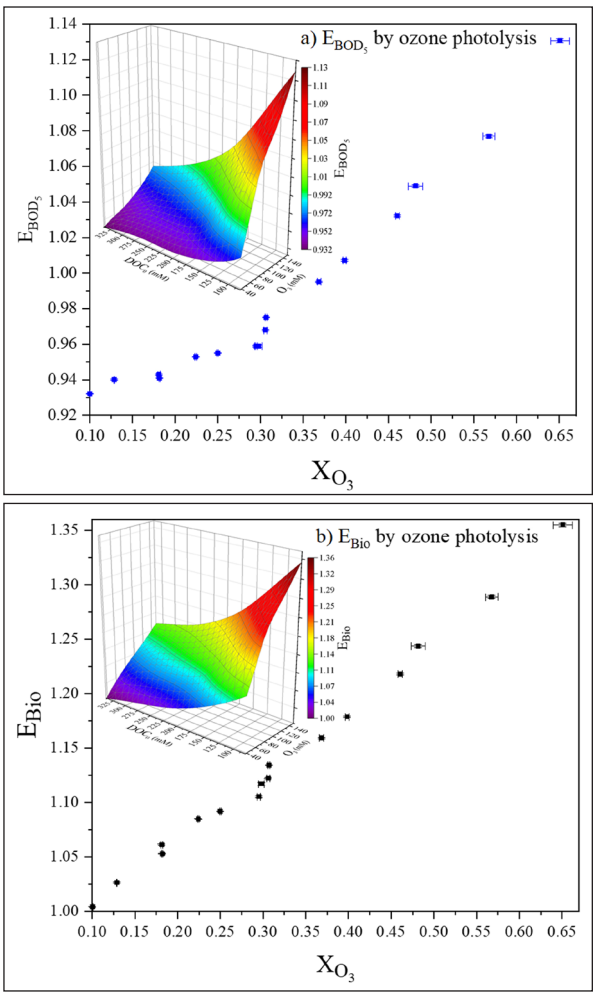


**Figure 5.** Effect of $O_3$ dosage molar ratio ($X_{O3}$) on the change of $BOD_5$ ($E_{BOD5}$) and biodegradability ($E_{bio}$) by ozone photolysis, the insets show the 3D surface plots of $E_{BOD5}$ and $E_{bio}$ as a function of $O_3$ dosage and $DOC_0$ value.

### *4.3. Treatment by $H_2O_2$/Dark and $H_2O_2$/UVA*

The effect of $H_2O_2$ dosage and initial organic content on OMW treatment was evaluated in the dark and under UVA irradiation by applying $H_2O_2$ doses from 66.7 to 266.7 mM on diluted OMW with initial organic content ($DOC_0$) ranged from 83.3 to 333.3 mM. The change in DOC, $BOD_5$, and biodegradability was presented by 3D surface plots (insets of the figures in this section) and 2D plots as a function of $H_2O_2$ dosage molar fraction ($X_{H2O2}$) and will be discussed based on that. Different from ozonation, it is more common by researchers to represent the efficiency in $H_2O_2$-based treatment using the ratio of $H_2O_2$ dose to the organic content measured as DOC (Souza et al., 2014), COD (Quispe-Arpasi et al., 2018), or TOC (Barrera et al., 2012). Similar to ozonation and ozone photolysis, the DOC reduction in $H_2O_2$/Dark and $H_2O_2$/UVA increased by increasing the $H_2O_2$ dosage or reducing $DOC_0$. As shown in Figure 6 a and b, it was possible to achieve 4.7% and 11.8% DOC reduction by $H_2O_2$/Dark and $H_2O_2$/UVA, respectively, under the best conditions. Nevertheless, the efficiency in both systems is low in comparison to the corresponding control experiments. The low capacity of $H_2O_2$ to cause a significant reduction in organic content is consistent with those published (Nie et al., 2010; Guo et al., 2018; Celeiro et al., 2018; Lamsal et al., 2011), where it is often linked to the low oxidation potential of $H_2O_2$ (Oturan and Aaron, 2014) and the high energy required to decompose it photolytically (Equation 5) (Dong et al., 2019; Celeiro et al., 2018).

Interestingly, the DOC reduction was paired with a significant change in $BOD_5$ (Figure 7 a and b), which indicates that DOC reduction in $H_2O_2$/Dark experiments is due only to the formed purgeable intermediates as no possible source of $OH^{\bullet}$ generation during the dark experiments is expected. In addition to the purgeable intermediate formation hypothesis, the DOC reduction in $H_2O_2$/UVA treatment is probably related to the photolysis of either the organics initially present in OMW or the generated oxidation intermediates and, to a lesser extent, to the $OH^{\bullet}$ generated from $H_2O_2$ photodecomposition (Equation 5). Despite that $H_2O_2$ decomposition requires UV irradiation in the range of 200 to 300 nm (Equation 5) (Oturan and Aaron, 2014), based on the absorption coefficient values in Lachheb et al. work (Lachheb et al., 2017), $H_2O_2$ can absorb up to 0.1 of the lamp emissions in the current study, which may result in a small amount of $OH^{\bullet}$ to be produced.

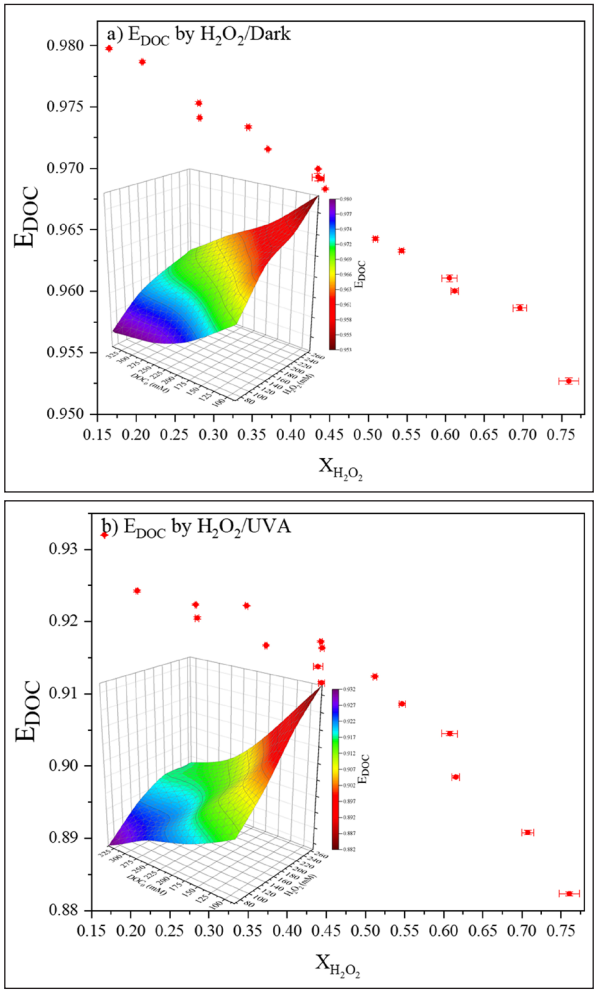


**Figure 6.** Effect of $H_2O_2$ dosage molar ratio ($X_{H2O2}$) on DOC reduction $E_{DOC}$) by; a) $H_2O_2$/Dark and b) $H_2O_2$/UVA, the insets show the 3D surface plots of $E_{DOC}$ as a function of $H_2O_2$ dosage and $DOC_0$ value.

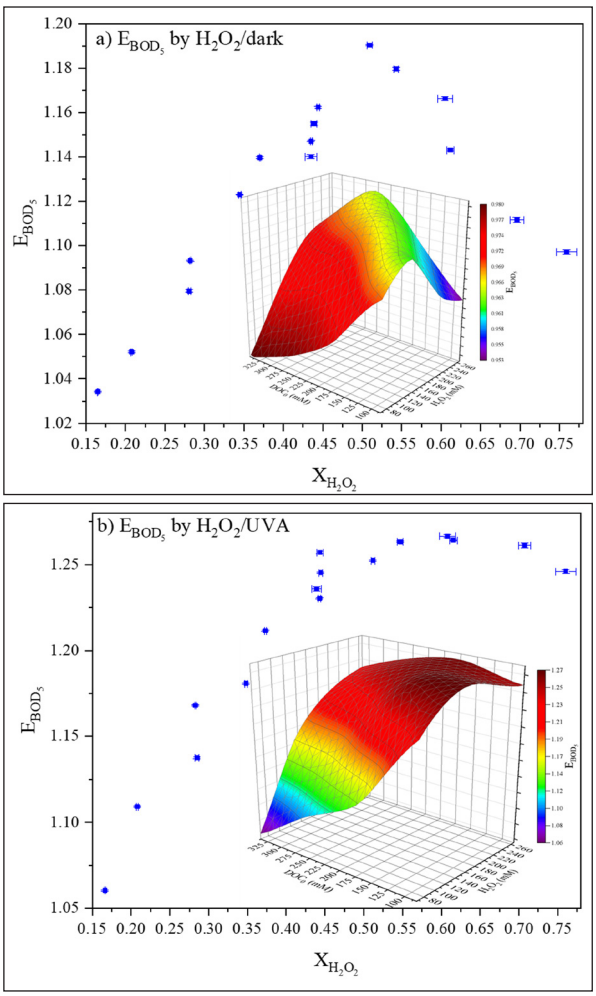


**Figure 7.** Effect of $H_2O_2$ dosage molar ratio ($X_{H2O2}$) on the change of $BOD_5$ ($E_{BOD5}$) by; a) $H_2O_2$/Dark and b) $H_2O_2$/UVA, the insets show the 3D surface plots of $E_{BOD5}$ as a function of $H_2O_2$ dosage and $DOC_0$ value.

In $H_2O_2$/Dark, $E_{BOD5}$ (Figure 7a) and $E_{bio}$ (Figure 8a) showed an upper optimum value at 0.51 $X_{H2O2}$ (1.19 and 1.23, $E_{BOD5,}$ and $E_{bio}$, respectively), which after this decreased dramatically. On the other hand, during $H_2O_2$/UVA treatment, $E_{BOD5}$ (Figure 7b) and $E_{bio}$ (Figure 8b) kept increasing with $X_{H2O2}$ to 0.6 (at which $E_{BOD5}$ = 1.27 and $E_{bio}$ = 1.42), above 0.6 $X_{H2O2}$, $E_{BOD5}$ slightly decreased while the $E_{bio}$ remained unchanged. The improvement in $BOD_5$ and biodegradability is due to the accumulation of the intermediates and their toxicity (Bar Oz et al., 2018; Khoufi et al., 2009), as explained before in ozonation.

### *4.4. Peroxonation and UVA/peroxonation*

The peroxonation and UVA/peroxonation treatment was carried out by applying different combinations of $H_2O_2$ and $O_3$ dosages (83.3 to 333.3 mM and 37.5-150 mM, respectively) on diluted OMW with different initial organic content (83.3 to 333.3 mM). Those combinations produced $H_2O_2$: $O_3$ ratio of 0.44 - 7.1, $H_2O_2$: $DOC_0$ ratio of 0.19 - 3.18, and $O_3$: $DOC_0$ ratio of 0.11 - 1.87, which include even a wider range of the examined ratios in the literature (Miklos et al., 2018; Oturan and Aaron, 2014; Li et al., 2015; Englehardt et al., 2013). The $E_{DOC}$, $E_{BOD5}$, and $E_{bio}$ results were depicted against ozone and hydrogen peroxide molar fraction on 3D surface plots with XY projection to visualize all parameters' effect. It is noteworthy that the initial dissolved organic carbon molar fraction is implicitly represented in the plots by the complementary of $X_{O3}$ plus $X_{H2O2}$ to unity.

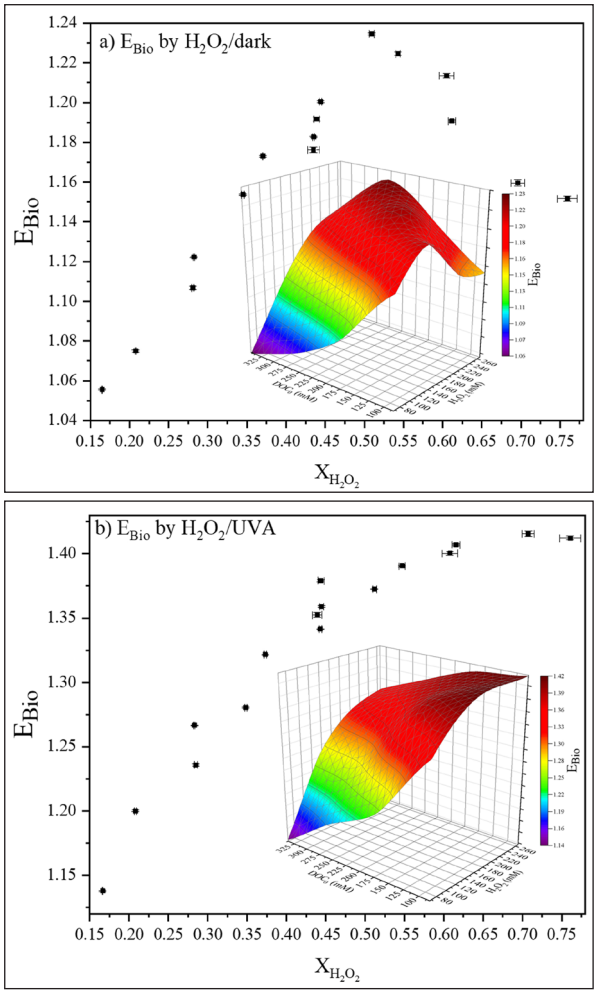


**Figure 8.** Effect of $H_2O_2$ dosage molar ratio ($X_{H2O2}$) on the change of biodegradability ($E_{bio}$) by; a) $H_2O_2$/Dark and b) $H_2O_2$/UVA, the insets show the 3D surface plots of $E_{bio}$ as a function of $H_2O_2$ dosage and $DOC_0$ value.

#### *4.4.1. Organic content reduction ($E_{DOC}$)*

As can be seen in Figure 9, the peroxonation and UVA peroxonation are more effective in DOC reduction than the treatment by ozone or hydrogen peroxide alone with or without UVA irradiation. The enhancement is mainly attributed to ozone decomposition by $H_2O_2$ (Equation 4) (Hassanshahi and Karimi-Jashni, 2018; Bethi et al., 2016; Wang and Xu, 2012). However, one shall keep in mind that the DOC reduction is caused by the complete mineralization and transforming the OMW organics into purgeable intermediates. The complete mineralization and intermediates formation involves synergistic and competitive pathways that can enhance or inhibit the DOC reduction efficiency. The main two competitive pathways include the $OH^{\bullet}$ scavenging by $H_2O_2$ (Equation 6) (Englehardt et al., 2013; Kurniawan and Lo, 2009) or $O_3$ (Equation 7) (Barzegar et al., 2019) and the interaction of oxidants with organic matters (Englehardt et al., 2013).

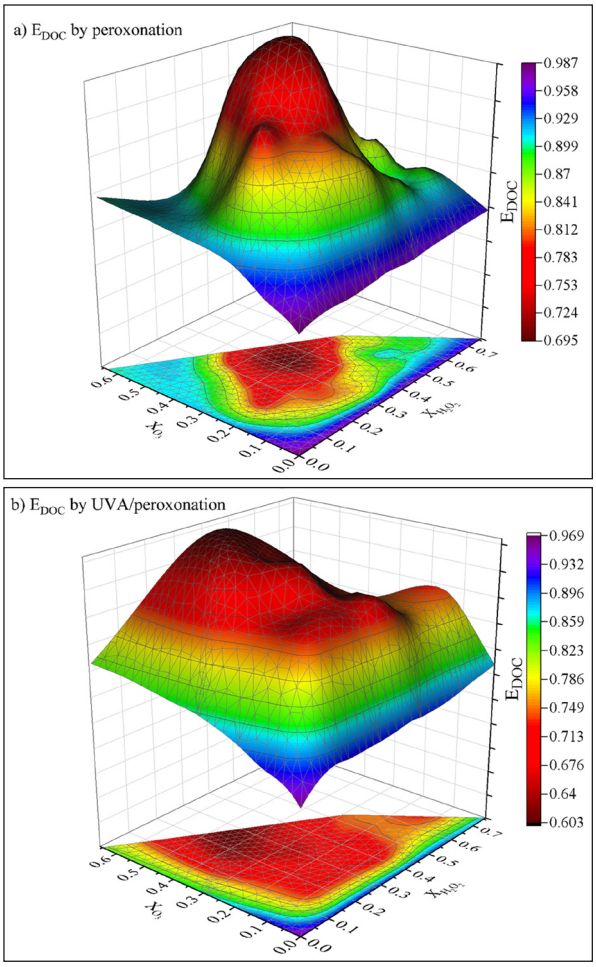


**Figure 9.** Effect of $H_2O_2$ and $O_3$ molar ratios ($X_{H2O2}$ and $X_{O3}$) and the initial dissolved organic carbon ($DOC_0$) concentration on DOC reduction ($E_{DOC}$) by; a) peroxonation, b) UVA/peroxonation.

Theoretically, the optimum $H_2O_2$: $O_3$ molar ratio to generate $OH^{\bullet}$ is 1:2 (Englehardt et al., 2013). However, several different ratios were obtained in this study. In peroxonation, the highest DOC reduction (≈ 30%) was between 0.28 - 0.4 $X_{H2O2}$ and 0.25 - 0.4 $X_{O3}$, which corresponds to 0.7 – 1.6 $H_2O_2$: $O_3$ molar ratio. On the other hand, the DOC reduction in UVA/peroxonation was higher than peroxonation alone, where ≈ 40% DOC reduction was achieved with a shift in the preferred $X_{H2O2}$ and $X_{O3}$ range to 0.18 - 0.32 and 0.33 – 0.5 (corresponds to 0.22 – 0.97 $H_2O_2$: $O_3$ molar ratio), respectively. The enhancement in UVA/peroxonation is expected because of the organics photolysis and the $OH^{\bullet}$ generated from $H_2O_2$ and $O_3$ photodecomposition (Equation 3 and Equation 5). Nevertheless, in UVA/peroxonation, it was possible to achieve more than 35% DOC reduction in all experiments regardless of the ozone or hydrogen peroxide molar ratio.

#### *4.4.2. Change in $BOD_5$ and biodegradability*

The OMW $BOD_5$ value for peroxonation treatment (Figure 10a) showed a substantial increase relative to treatment with ozone or hydrogen peroxide separately, where approximately more than 1.4% $E_{BOD5}$ was obtained for the whole tested range except for those with $X_{H2O2}$ > 0.5. Moreover, the maximum increase in the biodegradable fraction ($E_{BOD5}$ values > 2) was achieved in two distinct intervals of ozone and hydrogen peroxide molar ratios; 1) between 0.08 - 0.2 $X_{H2O2}$ and 0.1 - 0.4 $X_{O3}$, and 2) between 0.08 - 0.4 $X_{H2O2}$ and 0.1 - 0.2 $X_{O3}$. On the one hand, $E_{bio}$ in peroxonation (Figure 10b) increased over the whole range with a maximum value of 2.54. Nevertheless, it was possible to achieve about 100% enhancement in biodegradability for all $X_{H2O2}$ and $X_{O3}$ between 0.1- 0.4. As the optimal $O_3$ and $H_2O_2$ range for biodegradability enhancement are completely different from the optimal range for DOC reduction, it can be inferred that $BOD_5$ enhancement is due to direct oxidation by $H_2O_2$ and $O_3$, which did not contribute to mineralization or the formation of purgeable intermediates but rather caused accumulation of biodegradable intermediates.

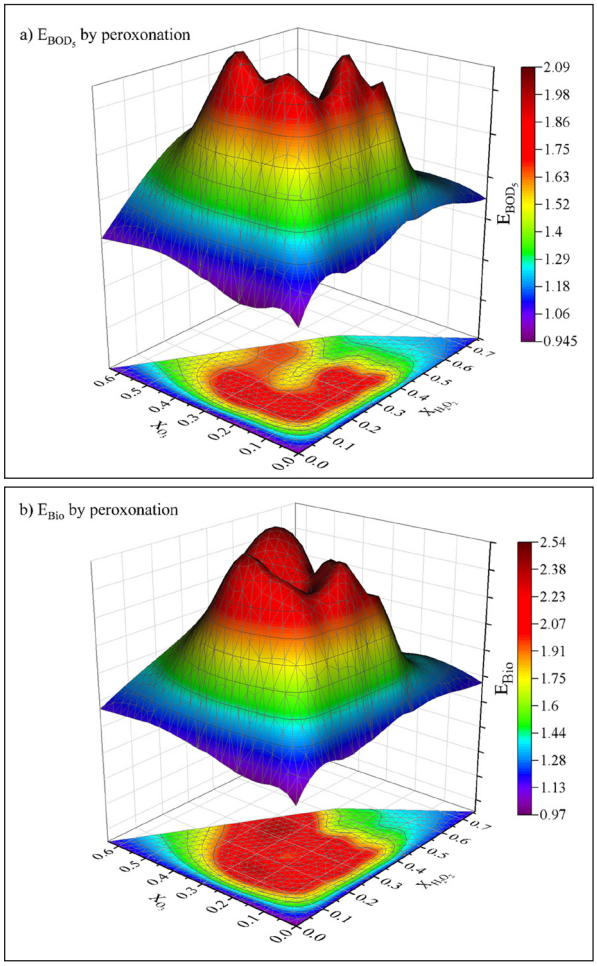


**Figure 10.** Effect of $H_2O_2$ and $O_3$ molar ratios ($X_{H2O2}$ and $X_{O3}$) and the initial dissolved organic carbon ($DOC_0$) concentration during peroxonation on; a) the change in $BOD_5$ ($E_{BOD5}$) and b) the change in biodegradability ($E_{bio}$).

On the other hand, UVA/peroxonation was less efficient in improving OMW biodegradable content (Figure 11a) or improving the biodegradability (Figure 11b) in comparison to peroxonation, where it showed a maximum of 1.38 and 2.12 $E_{BOD5}$ and $E_{bio}$, respectively. The lower efficiency implies that UVA/peroxonation has a higher affinity to attacks the biodegradable compounds. As can be seen from the same figure (Figure 11a), improving $E_{BOD5}$ is favoring $X_{H2O2}$ > 0.2 and $X_{O3}$< 0.5, which is the same range for biodegradability enhancement (Figure 11b). The use of very high doses of ozone ($X_{O3}$ > 0.5) has a detrimental effect on OMW's biodegradable fraction. Even though ozone removes refractory phenolic compounds, thus improving $E_{BOD5}$ by

decomposing the polyphenolic chain into smaller molecules, it may also generate numerous intermediates, which may disrupt the bacterial population within OMW (Bar Oz et al., 2018; Khoufi et al., 2009). It is worth to mention that even with the high biodegradability improvement by peroxonation and UVA/peroxonation, the final OMW biodegradability in any system never exceeded 0.67 (measured by $BOD_5$/TOC).

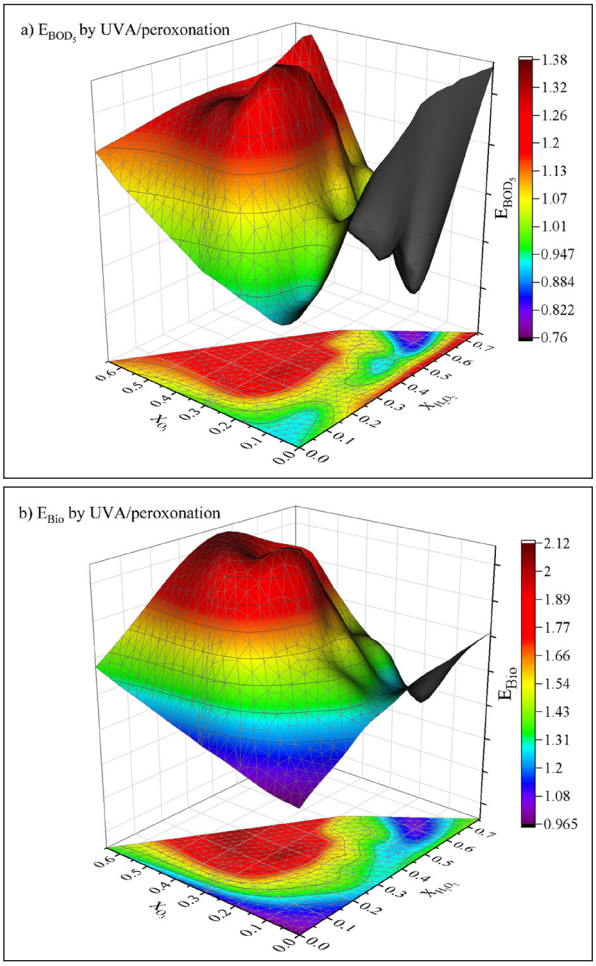


**Figure 11.** Effect of $H_2O_2$ and $O_3$ molar ratios ($X_{H2O2}$ and $X_{O3}$) and the initial dissolved organic carbon ($DOC_0$) concentration during UVA/peroxonation on; a) the change in $BOD_5$ ($E_{BOD5}$) and b) the change in biodegradability ($E_{bio}$).

## 5. Conclusions

Photolysis, ozonation ($O_3$/dark), ozone photolysis ($O_3$/UVA), $H_2O_2$-peroxidation ($H_2O_2$/Dark), $H_2O_2$ photo-peroxidation ($H_2O_2$/UVA), peroxonation ($H_2O_2$/$O_3$/dark), and photo-peroxonation ($H_2O_2$/$O_3$/UVA) were employed for OMW treatment. Using hydrogen peroxide as standalone or in combination with UVA irradiation showed to be infeasible for OMW DOC reduction. However, it could be a good choice for biodegradability enhancement, particularly under UVA irradiation. In ozonation and UVA ozonation, increasing the ozone dosage or reducing the initial OMW organic content enhanced the treatment efficiency. UVA/peroxonation showed the highest DOC reduction, while peroxonation showed the highest improvement in biodegradability. The combination of $H_2O_2$, $O_3$, and UVA has a synergetic and competitive effect on OMW organic content reduction and biodegradability change. However, the ratios of $H_2O_2$, $O_3$, and $DOC_0$ have numerous effects on OMW treatment efficiency. The appropriate ratio estimation is essential to wither apply the studied processes as an alternative or complementary treatment. This study also provides clear and valuable information regarding applying the tested systems as a pre or post-treatment when combined with other technologies according to the specific needs. For example, UVA peroxonation has high efficiency in reducing the organic content, making it more suitable as a polishing step for the biological treatment effluent. On the other hand, peroxonation significantly enhanced OMW biodegradability, making it a right pretreatment choice to improve biological wastewater treatment.

It was impossible to run this number of experiments under real sun conditions during the same milling campaign period in this stage of the project. Further experiments will be carried out in the second stage of the project to optimize OMW mineralization and biodegradability and to confirm the practical feasibility of tested systems under solar irradiation.

## References

Ahmed, P. M., Fernández, P.M., de Figueroa, L.I.C., Pajot, H. F. (2019). Exploitation Alternatives of Olive Mill Wastewater: Production of Value-Added Compounds Useful for Industry and Agriculture. Biofuel Research Journal 6: 980-94.

Akdemir, E. O., and Ozer, A. (2009). Investigation of Two Ultrafiltration Membranes for Treatment of Olive Oil Mill Wastewater. Desalination 249: 660-66.

Al-Bsoul, A., Al-Shannag, M., Tawalbeh, M., Al-Taani, A. A., Lafi, W. K., Al-Othman, A., Alsheyab, M. (2020). Optimal Conditions for Olive Mill Wastewater Treatment Using Ultrasound and Advanced Oxidation Processes. Science of the Total Environmen 700: 134576.

Ali, H., Iqbal, M. A., Atta, B. M., Ullah, R., Khan, M. B. (2020). Phenolic Profile and Thermal Stability of Monovarietal Extra Virgin Olive Oils Based on Synchronous Fluorescence Spectroscopy. Journal of Fluorescence 30: 939-47.

Alrousan, D. M. A. and Dunlop, P. S. M. (2020). Evaluation of Ozone-Based Oxidation and Solar Advanced Oxidation Treatment of Greywater. Journal of Environmental Chemical Engineering 8(5) 104309. https://doi.org/10.1016/j.jece.2020.104309

Amor, C., Marchão, L., Lucas, M.S., Peres, J.A. (2019). Application of Advanced Oxidation Processes for the Treatment of Recalcitrant Agro-Industrial Wastewater: A Review. Water 11(2), 205; https://doi.org/10.3390/w11020205

Andreozzi, R., Canterino, M., Somma, I. Di., Giudice, R. Lo., Marotta, R., Pinto, G., Pollio, A. (2008). Effect of Combined Physico-Chemical Processes on the Phytotoxicity of Olive Mill Wastewaters. Water Research 42(6-7): 1684-1692. https://doi.org/10.1016/j.watres.2007.10.018.

da Silva, D.A., Cavalcante, R. P., Cunha, R. F., Junior, A. M., de Oliveira, S. C. (2018). Optimization of Nimesulide Oxidation Via a Uv-Abc/H2o2 Treatment Process: Degradation Products, Ecotoxicological Effects, and Their Dependence on the Water Matrix. Chemosphere 207: 457-68.

Azbar, N., Bayram, A., Filibeli, A., Muezzinoglu, A., Sengul, F., Ozer, A. (2004). A Review of Waste Management Options in Olive Oil Production. Critical Reviews in Environmental Science and Technology 34: 209-47.

Azzam, M.O. J., Al-Gharabli, S.I., Al-Harahsheh, M.S. (2013). Olive Mills Wastewater Treatment Using Local Natural Jordanian Clay. Desalination and Water Treatment 53: 627-36.

Oz, Y. B., Mamane, H., Menashe, O., Cohen-Yaniv, V., Kumar, R., Kruh, L. I., Kurzbaum, E. (2018). Treatment of Olive Mill Wastewater Using Ozonation Followed by an Encapsulated Acclimated Biomass. Journal of Environmental Chemical Engineering 6: 5014-23.

Barrera, M., Mehrvar, M., Gilbride, K.A., McCarthy, L. H., Laursen, A. E., Bostan, V., Pushchak, R. (2012). Photolytic Treatment of Organic Constituents and Bacterial Pathogens in Secondary Effluent of Synthetic Slaughterhouse Wastewater. Chemical Engineering Research and Design 90: 1335-50.

Barzegar, G., Wu, J., Ghanbari, F. (2019). Enhanced Treatment of Greywater Using Electrocoagulation/Ozonation: Investigation of Process Parameters. Process Safety and Environmental Protection 121: 125-32.

Bertin, L., Berselli, S., Fava, F., Petrangeli-Papini, M., Marchetti, L. (2004). Anaerobic Digestion of Olive Mill Wastewaters in Biofilm Reactors Packed with Granular Activated Carbon and "Manville" Silica Beads. Water Research 38: 3167-78.

Bethi, B., Sonawane, S.H., Bhanvase, B. A., Gumfekar, S. P. (2016). Nanomaterials-Based Advanced Oxidation Processes for Wastewater Treatment: A Review. Chemical Engineering and Processing - Process Intensification 109: 178-89.

Marc-Olivier, B., Jochen, S., Sébastien, M., Martin, J., von Gunten, U.. (2006). Ozonation and Advanced Oxidation of Wastewater: Effect of O3 Dose, pH, DOM and HO• -Scavengers on Ozone Decomposition and HO• Generation. Ozone: Science and Engineering 28: 247-59.

Bustos-Terrones, Y., Rangel-Peraza, J. G., Sanhouse, A., Bandala, E. R., Torres, L. G. (2016). Degradation of Organic Matter from Wastewater Using Advanced Primary Treatment by O3 and O3/UV in a Pilot Plant. Physics and Chemistry of the Earth, Parts A/B/C, 91: 61-67.

Celeiro, M., Hackbarth, F. V., de Souza, S. M. A. G. U., Llompart, M., Vilar, V. J. P. (2018). Assessment of Advanced Oxidation Processes for the Degradation of Three UV Filters from Swimming Pool Water. Journal of Photochemistry and Photobiology A: Chemistry 351: 95-107.

Daghrir, R., Gherrou, A., Noel, I., Seyhi, B. (2016). Hybrid Process Combining Electrocoagulation, Electroreduction, and Ozonation Processes for the Treatment of Grey Wastewater in Batch Mode. Journal of Environmental Engineering 142: 04016008.

Dai, Q., Chen, L., Chen, W., Chen, J. (2015). Degradation and Kinetics of Phenoxyacetic Acid in Aqueous Solution by Ozonation. Separation and Purification Technology 142: 287-92. https://doi.org/10.1016/j.seppur.2014.12.045.

Dong, W., Sun, S-P., Yang, X., Zhou, K., Li, Y., Wang, X., Wu, Z., Wu, W. D., Chen, X D. (2019). Enhanced Emerging Pharmaceuticals Removal in Wastewater after Biotreatment by a Low-Pressure UVA/Feiii-EDDS/H2O2 Process under Neutral pH Conditions. Chemical Engineering Journal 366: 539-49.

Ebrahimi, Izadyar, Mazeyar Parvinzadeh Gashti, Mojtaba Sarafpour. (2018). Photocatalytic Discoloration of Denim Using Advanced Oxidation Process with H2O2/UV. Journal of Photochemistry and Photobiology A: Chemistry 360: 278-88.

El-Abbassi, A., A. Hafidi, M. Khayet, M. C. García-Payo. (2013). Integrated Direct Contact Membrane Distillation for Olive Mill Wastewater Treatment. Desalination 323: 31-38.

Elmolla, Emad S., Malay Chaudhuri. (2010). Photocatalytic Degradation of Amoxicillin, Ampicillin and Cloxacillin Antibiotics in Aqueous Solution Using UV/TiO2 and UV/H2O2/TiO2 Photocatalysis. Desalination 252: 46-52.

Englehardt, J. D., T. Wu, G. Tchobanoglous. (2013). Urban Net-Zero Water Treatment and Mineralization: Experiments, Modeling and Design Water Research 47: 4680-91.

Erses Yay, A. Suna, H. Volkan Oral, Turgut T. Onay, Orhan Yenigün. (2012). A Study on Olive Oil Mill Wastewater Management in Turkey: A Questionnaire and Experimental Approach, Resources. Conservation and Recycling 60: 64-71.

Farzadkia, Mahdi, Yousef Dadban Shahamat, Simin Nasseri, Amir Hossein Mahvi, Mitra Gholami, Ali Shahryari. (2014). Catalytic Ozonation of Phenolic Wastewater: Identification and Toxicity of Intermediates. Journal of Engineering 2014: 1-10.

García, Cristina Agabo, Gassan Hodaifa. (2017). Real Olive Oil Mill Wastewater Treatment by Photo-Fenton System Using Artificial Ultraviolet Light Lamps. Journal of Cleaner Production 162: 743-53.

Gardoni, D., A. Vailati, R. Canziani. (2012). Decay of Ozone in Water: A Review. Ozone: Science & Engineering 34: 233-42.

Gulyas, H., H. B. Jain, A. L. Susanto, M. Malekpur, K. Harasiuk, I. Krawczyk, P. Choromanski, M. Furmanska. (2005). Solar Photocatalytic Oxidation of Pretreated Wastewaters: Laboratory Scale Generation of Design Data for Technical-Scale Double-Skin Sheet Reactors. Environmental Technology 26: 501-14.

Guo, K., Z. Wu, S. Yan, B. Yao, W. Song, Z. Hua, X. Zhang, X. Kong, X. Li, J. Fang. (2018). Comparison of the UV/Chlorine and UV/H2O2 Processes in the Degradation of Ppcps in Simulated Drinking Water and Wastewater: Kinetics, Radical Mechanism and Energy Requirements. Water Research 147: 184-94.

Hassanshahi, N., and A. Karimi-Jashni. (2018). Comparison of Photo-Fenton, O3/H2O2/UV and Photocatalytic Processes for the Treatment of Gray Water. Ecotoxicology and Environmental Safety 161: 683-90.

Hodaifa, G., Gallardo, P. A. R., García, C. A., Kowalska, M., Seyedsalehi, M. (2019). Chemical Oxidation Methods for Treatment of Real Industrial Olive Oil Mill Wastewater. Journal of the Taiwan Institute of Chemical Engineers 97: 247-54.

Huang, W., Bianco, A., Brigante, M., Mailhot, G. (2018). Uva-Uvb Activation of Hydrogen Peroxide and Persulfate for Advanced Oxidation Processes: Efficiency, Mechanism and Effect of Various Water Constituents. Journal of Hazardous Materials 347: 279-87.

Iboukhoulef, H., Douani, R., Amrane, A., Chaouchi, A., Elias, A. (2019). Heterogeneous Fenton Like Degradation of Olive Mill Wastewater Using Ozone in the Presence of BiFeO3 Photocatalyst. Journal of Photochemistry and Photobiology A: Chemistry, 383. Elsevier, 2019, 383, □10.1016/j.jphotochem.2019.112012□. □hal-02359982□.

Ioannou-Ttofa, L., Michael-Kordatou, I., Fattas, S. C., Eusebio, A., Ribeiro, P., M. Rusan, A. R. Amer, S. Zuraiqi, M. Waismand, C. Linder, Z. Wiesman, J. Gilron, D. Fatta-Kassinos. (2017). Treatment Efficiency and Economic Feasibility of Biological Oxidation, Membrane Filtration and Separation Processes, and Advanced Oxidation for the Purification and Valorization of Olive Mill Wastewater. Water Research 114: 1-13.

Kasprzyk-Hordern, B., Ziółek, M., Nawrocki, J. (2003). Catalytic Ozonation and Methods of Enhancing Molecular Ozone Reactions in Water Treatment. Applied Catalysis B: Environmental 46: 639-69.

Khataee, A., Kıranşan, M, Karaca, S., Sheydaei, M. (2017). Photocatalytic Ozonation of Metronidazole by Synthesized Zinc Oxide Nanoparticles Immobilized on Montmorillonite. Journal of the Taiwan Institute of Chemical Engineers 74: 196-204.

Khoufi, S., Aloui, F., Sayadi, S. (2009). Pilot Scale Hybrid Process for Olive Mill Wastewater Treatment and Reuse, Chemical Engineering and Processing: Process Intensification 48: 643-50.

Kurniawan, T. A., and Lo, W. H. (2009). Removal of Refractory Compounds from Stabilized Landfill Leachate Using an Integrated H2O2 Oxidation and Granular Activated Carbon (Gac) Adsorption Treatment. Water Research 43: 4079-91.

Lachheb, H., Guillard, C., Lassoued, H., Haddaji, M., Rajah, M., Houas, A. (2017). Photochemical Oxidation of Styrene in Acetonitrile Solution in Presence of H2O2, TiO2 /H2O2 and Zno/H2o2. Journal of Photochemistry and Photobiology A: Chemistry 346: 462-69.

Lafi, W. K., Shannak, B., Al-Shannag, M., Al-Anber, Z., Al-Hasan, M. (2009). Treatment of Olive Mill Wastewater by Combined Advanced Oxidation and Biodegradation. Separation and Purification Technology 70: 141-46.

Lamsal, R., Walsh, M. E., Gagnon, G. A. (2011). Comparison of Advanced Oxidation Processes for the Removal of Natural Organic Matter. Water Researc, 45: 3263-9.

Li, G.; He, J.; Wang, D.; Meng, P.; Zeng, M. (2015). Optimization and Interpretation of O3 and O3/H2O2 Oxidation Processes to Pretreat Hydrocortisone Pharmaceutical Wastewater. Environmental Technology 36: 1026-34.

Michael-Kordatou, I., Karaolia, P. Fatta-Kassinos, D. (2018). The Role of Operating Parameters and Oxidative Damage Mechanisms of Advanced Chemical Oxidation Processes in the Combat against Antibiotic-Resistant Bacteria and Resistance Genes Present in Urban Wastewater. Water Research 129: 208-30.

Miklos, D. B., Remy, C., Jekel, M., Linden, K. G., Drewes, J. E., Hubner, U. (2018). Evaluation of Advanced Oxidation Processes for Water and Wastewater Treatment - a Critical Review. Water Research 139: 118-31.

Miranda, M.A., Amat, A.M., Arques, A. (2001). Abatement of the Major Contaminants Present in Olive Oil Industry Wastewaters by Different Oxidation Methods: Ozone and/or Uv Radiation Versus Solar Light. Water Science and Technology 44: 325-30.

Moreira, N. F. F., Narciso-da-Rocha, C., Polo-Lopez, M. I., Pastrana-Martinez, L. M., Faria, J. L., Manaia, C. M., Fernandez-Ibanez, P., Nunes, O. C., Silva, A. M. T. (2018). Solar Treatment (H2o2, TiO2-P25 and Go-TiO2 Photocatalysis, Photo-Fenton) of Organic Micropollutants, Human Pathogen Indicators, Antibiotic Resistant Bacteria and Related Genes in Urban Wastewater. Water Research 135: 195-206.

Nguyen, A. T., and Juang, R. S. (2015). Photocatalytic Degradation of P-Chlorophenol by Hybrid H2O2 and TiO2 in Aqueous Suspensions under UV Irradiation. Journal of Environmental Management 147: 271-7.

Niazmand, R., Jahani, M., Sabbagh, F., Rezania, S. (2020). Optimization of Electrocoagulation Conditions for the Purification of Table Olive Debittering Wastewater Using Response Surface Methodology. Water 12. 12(6), 1687; https://doi.org/10.3390/w12061687.

Nie, Y., Hu, C. Zhou, L., Qu, J., Wei, Q., Wang, D. (2010). Degradation Characteristics of Humic Acid over Iron Oxides/Fe0 Core-Shell Nanoparticles with UVA/H2O2. Journal of Hazardous Materials 173: 474-9.

Ochando-Pulido, J. M., Pimentel-Moral, S., Verardo, V., Martinez-Ferez, A. (2017). A Focus on Advanced Physico-Chemical Processes for Olive Mill Wastewater Treatment. Separation and Purification Technology 179: 161-74.

Otálvaro-Marín, H. L., González-Caicedo, F., Arce-Sarria, A., Mueses, M. A., Crittenden, J. C., Machuca-Martinez, F. (2019). Scaling-up a Heterogeneoush2o2/Tio2/Solar-Radiation System Using the Damköhler Number. Chemical Engineering Journal 364: 244-56. https://doi.org/10.1016/j.cej.2019.01.141.

Oturan, M. A., and Aaron, J-J. (2014). Advanced Oxidation Processes in Water/Wastewater Treatment: Principles and Applications. A Review. Critical Reviews in Environmental Science and Technology 44(23): 2577-641. DOI:10.1080/10643389.2013.829765

Pedrero, F., Grattan, S. R., Ben-Gal, A., Vivaldi, G A. (2020). Opportunities for Expanding the Use of Wastewaters for Irrigation of Olives. Agricultural Water Management 241. https://doi.org/10.1016/j.agwat.2020.106333.

Pérez-Lucas, G., Aliste, M., Vela, N., Garrido, I., Fenoll, J., Navarro, S. (2020). Decline of Fluroxypyr and Triclopyr Residues from Pure, Drinking and Leaching Water by Photo-Assisted Peroxonation. Process Safety and Environmental Protection 137: 358-65.

Quispe-Arpasi, D., Souza, R. de, Stablein, M., Liu, Z., Duan, N., Lu, H., Zhang, Y., Alessandra, A. L. de O., Ribeiro, R., Tommaso, G. (2018). Anaerobic and Photocatalytic Treatments of Post-Hydrothermal Liquefaction Wastewater Using H2o2, Bioresource Technology Reports, 3: 247-55. https://doi.org/10.1016/j.biteb.2018.08.003.

Saez, J. A., M. D. Perez-Murcia, A. Vico, M. R. Martinez-Gallardo, F. J. Andreu-Rodriguez, M. J. Lopez, M. A. Bustamante, J. C. Sanchez-Hernandez, J. Moreno, R. Moral. (2020). Olive Mill Wastewater-Evaporation Ponds Long Term Stored: Integrated Assessment of in Situ Bioremediation Strategies Based on Composting and Vermicomposting. Journal of Hazardous Materials 402: 123481.

Souza, B. S., Dantas, R. F., Cruz, A., Sans, C., Esplugas, S., Dezotti, M. (2014). Photochemical Oxidation of Municipal Secondary Effluents at Low H2O2 Dosage: Study of Hydroxyl Radical Scavenging and Process Performance. Chemical Engineering Journal 237: 268-76. https://doi.org/10.1016/j.cej.2013.10.025

Uğurlu, M., Yilmaz, S. İ., Vaızoğuiiar, A. (2019). Removal of Color and Cod from Olive Wastewater by Using Three-Phase Three-Dimensional (3d) Electrode Reactor, Materials Today: Proceedings, 18: 1986-95.

Wang, J. L., and Xu, L. J. (2012). Advanced Oxidation Processes for Wastewater Treatment: Formation of Hydroxyl Radical and Application. Critical Reviews in Environmental Science and Technology 42: 251-325. DOI:10.1080/10643389.2010.507698

Wert, E. C., Rosario-Ortiz, F. L., Snyder, S. A. (2009). Effect of Ozone Exposure on the Oxidation of Trace Organic Contaminants in Wastewater. Water Research 43: 1005-14.

Yazdanbakhsh, A., Mehdipour, F., Eslami, A., Maleksari, H. S., Ghanbari, F. (2015). The Combination of Coagulation, Acid Cracking and Fenton-Like Processes for Olive Oil Mill Wastewater Treatment: Phytotoxicity Reduction and Biodegradability Augmentation, Water Science and Technology, 71(7): 1097-105.

Yuval, A., Eran, F., Janin, W., Oliver, O., Yael, D. (2017). Photodegradation of Micropollutants Using V-UV/UV-C Processes; Triclosan as a Model Compound, Science of the Total Environment, 601-602: 397-404.